Determination of the Rate of Reduction of Oxyferrous Cytochrome P450 2B4 by 5-Deazariboflavin Adenine Dinucleotide T491V Cytochrome P450 Reductase†

Haoming Zhang,‡ Larry Gruenke,‡ Dave Arscott,‡ Anna Shen,⊥ Charles Kasper,⊥ Danni L. Harris,§ Michael Glavanovich,∥ Richard Johnson,∥ and Lucy Waskell*,‡

University of Michigan and VA Medical Research Center, 2215 Fuller Road, Ann Arbor, Michigan 48105, McArdle Laboratory for Cancer Research, University of Wisconsin, Madison, Wisconsin 53706, Molecular Research Institute, 2495 Old Middlefield Way, Mountain View, California 94043, and Avtech Laboratories, Inc., 68959 Quality Way, Kalamazoo, Michigan 49002

Received June 5, 2003; Revised Manuscript Received August 12, 2003

ABSTRACT: The use of 5-deazaFAD T491V cytochrome P450 reductase has made it possible to directly measure the rate of electron transfer to microsomal oxyferrous cytochrome (cyt) P450 2B4. In this reductase the FMN moiety can be reduced to the hydroquinone, $FMNH_2$, while the 5-deazaFAD moiety remains oxidized [Zhang, H., et al. (2003) *Biochemistry 42*, 6804−6813]. The rate of electron transfer from 5-deazaFAD cyt P450 reductase to oxyferrous cyt P450 was determined by rapidly mixing the ferrous cyt P450−2-electron-reduced 5-deazaFAD T491V reductase complex with oxygen in the presence of substrate. The 5-deazaFAD T491V reductase which can only donate a single electron reduces the oxyferrous cyt P450 and oxidizes to the air-stable semiquinone, with rate constants of 8.4 and 0.37 s^{-1} at 15 °C. Surprisingly, oxyferrous cyt P450 turns over more slowly with a rate constant of 0.09 s^{-1}, which is the rate of catalysis under steady-state conditions at 15 °C ($k_{cat} = 0.08\ s^{-1}$). In contrast, the rate constant for electron transfer from ferrous cyt b_5 to oxyferrous cyt P450 is 10 s^{-1} with oxyferrous cyt P450 and cyt b_5 simultaneously undergoing spectral changes. Quantitative analyses by LC-MS/MS revealed that the product, norbenzphetamine, was formed with a coupling efficiency of 52% with cyt b_5 and 32% with 5-deazaFAD T491V reductase. Collectively, these results suggest that during catalysis a relatively stable reduced oxyferrous intermediate of cyt P450 is formed in the presence of cyt P450 reductase but not cyt b_5 and that the rate-limiting step in catalysis follows introduction of the second electron.

The cytochromes P450 are a ubiquitous superfamily of mixed function oxidases which function primarily as monooxygenases (*1*, *2*). They play important catalytic roles in a number of vital processes including (1) biosynthesis of steroids, eicosanoids, and numerous other endogenous compounds, (2) generation of secondary metabolites and oxidation of organic compounds for use as an energy source in microorganisms, and (3) degradation and activation of xenobiotics which can have either beneficial or deleterious effects. Their commercial importance is based on their essential role in metabolizing a great variety of pharmaceutical compounds and on their potential utility in bioremediation where they effect the degradation of recalcitrant environmental contaminants. The cyt P450 catalyzed activation of oxygen requires two electrons and two protons and is generally considered to consist of the following processes: (1) binding of a substrate resulting in an increase in the reduction potential of the iron, (2) reduction of the ferric protein by cyt P450 reductase[1] (first electron), (3) binding of molecular oxygen to the ferrous protein, (4) transfer of a second electron from either cyt P450 reductase or cyt b_5, resulting in the formation of reduced oxyferrous cyt P450 which is also known as the peroxo intermediate $(Fe^{3+}OO)^{2-}$, (5) protonation on the distal oxygen to form a hydroperoxo intermediate $(Fe^{3+}OOH)^{-}$, (6) uptake of a second proton which facilitates O−O bond cleavage and leads irreversibly to water and an oxyferryl species $(FeO)^{3+}$, whose precise electronic configuration is unknown (the oxyferryl species is considered to be analogous to the relatively stable compound I in peroxidases; the iron is in the Fe^{4+} oxidation state and the porphyrin ring is a one-electron-deficient π-cation radical), (7) insertion of the oxyferryl oxygen, into the carbon−hydrogen bond of a substrate, and (8) dissociation of the product to regenerate the ferric resting state. The reactions describing formation of oxyferrous cyt P450, steps 1−3, and product dissociation, step 8, have been studied extensively in several systems and are known not to limit the overall rate of catalysis. However, steps 4−7, which include reduction and subsequent protonation of the oxyferrous cyt P450 and cleavage and insertion of the activated oxygen into substrate, are less well understood and are candidates for the rate-limiting step in catalysis (*3*−*6*). In the case of cyt $P450_{cam}$ the rate-determining step has been identified as reduction of oxyferrous cyt $P450_{cam}$ by puti-

† This work was supported by a National Institutes of Health Grant (GM35533) and a VA Merit Review Grant to L.W.

* To whom correspondence should be addressed. Phone: (734) 769-7100 ext 5858. Fax: (734) 213-6985. E-mail: waskell@umich.edu.

‡ University of Michigan and VA Medical Research Center.

⊥ University of Wisconsin.

§ Molecular Research Institute.

∥ Avtech Laboratories, Inc.

[1] Abbreviations: FAD, flavin adenine dinucleotide; FMN, flavin mononucleotide; 5-deazaFAD, 5-deazariboflavin adenine dinucleotide; cyt P450 reductase, NADPH−cytochrome P450 reductase; cyt P450, cytochrome P450; cyt b_5, cytochrome b_5; cyt *c*, cytochrome *c*; LC-MS/MS, liquid chromatography−mass spectrometry/mass spectrometry.

10.1021/bi034968u CCC: $25.00
Published on Web 09/20/2003

daredoxin (*7*). However, the rate of reduction of a microsomal oxyferrous cyt P450 by cyt P450 reductase has never been measured due to the lability of the microsomal oxyferrous cyts P450 and the ambiguities in interpreting the spectral changes which occur during oxidation of the diflavin reductase which has nine possible oxidation−reduction states (*8*). Although most of the reactions of cyt P450 can be rationalized by involving the participation of the high-valent, electrophilic FeO^{3+} species, some experiments have demonstrated that the peroxo and hydroperoxo species can catalyze nucleophilic and electrophilic reactions, respectively. Many scientists in the field have concluded that cyt P450 catalyzed hydroxylations may proceed via multiple oxidants and mechanisms (*9*).

In an effort to elucidate the molecular basis of how cyt b_5 stimulates the rate of metabolism and increases the efficiency of catalysis by cyt P450 2B4, we have compared the rate of reduction of oxyferrous cyt P450 2B4 by cyt b_5 and by cyt P450 reductase using a cyt P450 reductase preparation which is capable of delivering only a single electron from the FMN hydroquinone (*10*−*15*). The FMN semiquinone is air stable and does not reduce cyt P450. The wild-type diflavin reductase cannot be used for this purpose because the electrons are in rapid equilibrium and are distributed between the three oxidation states of each of the two flavins according to their redox potentials. The rapid reequilibration of electrons in a wild-type reductase molecule following loss of an electron from the protein gives rise to spectral changes which cannot be unambiguously deconvoluted. Cyt P450 reductase contains one molecule of FMN and FAD per polypeptide chain. NADPH transfers its electrons to FAD, which quickly reduces FMN. The FMN hydroquinone donates an electron to cyt P450 and other cytochromes such as cyt b_5 and cyt *c*. The T491V variant of cyt P450 reductase which binds FAD ∼100-fold less tightly than the wild-type protein could be reconstituted with 5-deazaFAD which has a potential of ∼−650 mV. The low potential prevents the 5-deazaFAD cofactor from being reduced under our experimental conditions (*16*, *17*). This 5-deazaFAD T491V reductase, in which only the FMN hydroquinone can donate a single electron, enabled us to measure, for the first time, the rate of reduction of a microsomal oxyferrous cyt P450 by a microsomal cytochrome P450 reductase and to compare it to the rate of reduction by cyt b_5. Our results demonstrate that under the experimental conditions oxyferrous cyt P450 2B4 and ferrous cyt b_5 undergo changes in oxidation state simultaneously; in contrast, under identical conditions oxyferrous cyt P450 2B4 and 5-deazaFAD reductase turn over at markedly different rates. The reductase oxidizes first and after ≅1 s cyt P450 begins to return to the ferric state. Oxyferrous cyt P450 reverts to the ferric state approximately 100-fold more slowly than the 2-electron-reduced 5-deazaFAD reductase, which oxidizes with the same rate constant as cyt b_5 and oxyferrous cyt P450 2B4 in the control experiment. These findings are interpreted to indicate that a reduced oxyferrous cyt P450 intermediate accumulates during catalysis in the presence of cyt P450 reductase but not cyt b_5 and that a reaction following delivery of the second electron is rate limiting. The more rapid turnover of cyt P450 2B4 in the presence of cyt b_5 compared to cyt P450 reductase diminishes the time available for uncoupling reactions and results in a more efficient catalytic reaction cycle.

MATERIALS AND METHODS

Materials. All chemicals used are of ACS grade unless otherwise specified. Benzphetamine, amphetamine sulfate, benzoyl-d_5 chloride, benzoyl chloride, lithium aluminum hydride, and sodium dithionite were purchased from Sigma-Aldrich (St. Louis, MO). Dilauroylphosphatidylcholine (DLPC) was purchased from Doosan Serdary Research Laboratory (Toronto, Canada). It is of note that impurities existing in commercial glycerol, even in spectrophotometric grade, are capable of reducing cyt b_5 under anaerobic conditions. Therefore, the glycerol used for all of the stopped-flow studies was distilled twice under vacuum to remove the impurities.

Preparation of Cyt P450 2B4, Cyt b_5, and 5-DeazaFAD T491V Reductase. Cyt P450 2B4 and cyt b_5 were expressed in *Escherichia coli* C41(DE3) and purified as previously described (*18*, *19*). 5-deazaFAD T491V reductase was prepared as described (*16*). Briefly, 5-deazaFAD was synthesized from 5-deazariboflavin. It was then used to replace the FAD in the T491V mutant of cyt P450 reductase by incubating the mutant reductase in the presence of excess 5-deazaFAD. The molar ratio of FMN to 5-deazaFAD in the reductase preparation varied from 0.96 to 1.2 depending on the particular reductase preparation. The concentration of cyt P450 2B4 was determined spectrophotometrically using an extinction coefficient of $\Delta\epsilon_{450-490nm}$ of 91 mM^{-1} cm^{-1} for the ferrous cyt P450−CO complex (*20*). The concentration of cyt b_5 was determined spectrophotometrically using an extinction coefficient of $\Delta\epsilon_{409-424nm}$ of 185 mM^{-1} cm^{-1} between reduced and oxidized cyt b_5 (*19*, *21*). The concentration of 5-deazaFAD T491V reductase was determined by measuring the absorbance of the oxidized FMN cofactor and using an $\epsilon_{450\ nm}$ of 9.1 mM^{-1} cm^{-1} (*16*).

Determination of the Rate of Autoxidation of Oxyferrous Cyt P450, Cyt b_5, and 5-DeazaFAD T491V Reductase. All kinetic studies were performed at 15 °C in a SF61DX2 stopped-flow spectrophotometer (Hi-Tech Co.) housed in a glovebox unless specified otherwise. Kinetic data were recorded either in the photodiode array (PDA) mode to obtain full spectra from 330 to 700 nm or in the photomultiplier mode to obtain absorbance changes at a single wavelength. Rate constants and amplitudes were obtained by fitting the absorbance change at a particular wavelength with multiple exponential functions using KinetAsyst2 software (Hi-Tech Co.).

The rate of autoxidation of oxyferrous cyt P450 was determined by incubating a deaerated solution of cyt P450 (5−10 μM) in buffer A (0.1 M potassium phosphate, 15% glycerol, pH 7.4) with a 60-fold molar excess of DLPC overnight at 4 °C in an anaerobic glovebox (Belle Technology, Portesham, Dorset, U.K.) to remove oxygen. Benzphetamine and methyl viologen were added anaerobically to a final concentration of 1 mM and 0.1 μM, respectively. Cyt P450 was then transferred to a tonometer and reduced to ferrous cyt P450 with a stoichiometric amount of a dithionite solution that had been standardized with a known amount of cyt b_5. The reduced cyt P450 was introduced into a syringe on the stopped-flow spectrophotometer and was rapidly mixed with anaerobic buffer B (buffer A plus 1 mM benzphetamine). Benzphetamine was included in buffer B to maintain a constant benzphetamine concentration in the

final reaction mixture. Loading the protein-containing solution into the stopped-flow spectrophotometer results in an ~6% dilution. This dilution was corrected by normalizing the spectrum of the reduced cyt P450 recorded in the tonometer to the spectrum recorded in the observation cell of the stopped-flow spectrophotometer. The kinetics of the autoxidation of oxyferrous cyt P450 were then followed at 438 nm [$\Delta\epsilon(Fe^{2+}O_2-Fe^{3+}) = 23\ mM^{-1}\ cm^{-1}$] after rapid mixing with air-saturated ([O_2] = 0.32 mM) buffer B. To determine the second-order rate constant for formation of oxyferrous cyt P450, ferrous cyt P450 was mixed under pseudo-first-order conditions with a series of solutions of buffer B containing different concentrations of oxygen. The oxygen concentration was varied by diluting air-saturated buffer B with anaerobic buffer B. Linear regression analysis of the apparent first-order rate constant k_{app} versus the concentration of oxygen yielded the second-order rate constant. The rate of autoxidation of cyt b_5 and 5-deazaFAD T491V cytochrome P450 reductase from the $FMNH_2$ to the air-stable $FMNH^{\bullet}$ at 15 °C was determined by mixing with air-saturated buffer as described for cyt P450 2B4.

Determination of the Rate of Electron Transfer from Ferrous Cyt b_5 to Oxyferrous Cyt P450 2B4. The rate of electron transfer from ferrous cyt b_5 to oxyferrous cyt P450 was determined by incubating an equal molar amount of cyt P450 and cyt b_5 in buffer A plus a 60-fold molar excess of DLPC overnight at 4 °C in an anaerobic glovebox. Benzphetamine and methyl viologen were added anaerobically to the cyt P450−cyt b_5 complex to a final concentration of 1 mM and 0.1 μM, respectively. This protein complex was then reduced with a stoichiometric amount of dithionite in a tonometer. The reduced complex was introduced into a syringe on the stopped-flow spectrophotometer and rapidly mixed with air-saturated buffer B. The kinetics of the electron transfer were followed at 438 nm [$\Delta\epsilon(Fe^{2+}O_2-Fe^{3+}) = 23\ mM^{-1}\ cm^{-1}$] for cyt P450 and 422 nm [$\Delta\epsilon(b_5{}^{2+}-b_5{}^{3+}) = 106\ mM^{-1}\ cm^{-1}$] for cyt b_5.

Determination of the Rate of Electron Transfer from 5-DeazaFAD T491V Reductase to Oxyferrous Cyt P450 2B4. The rate of electron transfer from 5-deazaFAD reductase to oxyferrous cyt P450 2B4 was determined using exactly the same procedures as used for cyt P450−cyt b_5 (see the section above). Briefly, an equal molar amount of cyt P450 and 5-deazaFAD reductase (5−10 μM) was incubated overnight in the glovebox at 4 °C in buffer A plus a 60-fold molar excess of DLPC to preform the cyt P450−5-deazaFAD reductase complex. After addition of benzphetamine and methyl viologen the protein complex was stoichiometrically reduced with dithionite. The stoichiometric reduction of the protein complex yielded ferrous cyt P450, and the 2-electron-reduced 5-deazaFAD reductase in which FMN was reduced to $FMNH_2$ and 5-deazaFAD remained oxidized. The 3-electron-reduced protein complex was loaded into the stopped-flow spectrophotometer and mixed with air-saturated buffer B. The intermolecular electron transfer between oxyferrous cyt P450 and 5-deazaFAD reductase was followed at 438 nm where oxyferrous cyt P450 shows maximal absorbance change when it decomposes to ferric cyt P450 [$\Delta\epsilon(Fe^{2+}O_2-Fe^{3+}) = 23\ mM^{-1}\ cm^{-1}$]. At 438 nm 5-deazaFAD reductase exhibits a small increase in absorbance ($\Delta\epsilon = 1.5\ mM^{-1}\ cm^{-1}$) as the $FMNH_2$ oxidizes to the $FMNH^{\bullet}$. The oxidation of 5-deazaFAD reductase was followed at 598 nm, which is an isosbestic point between oxyferrous cyt P450 and ferric cyt P450 ($\Delta\epsilon_{598\ nm} = 2.8\ mM^{-1}\ cm^{-1}$). In addition the transient spectra arising during electron transfer were recorded every 50 ms from 330 to 700 nm in the PDA mode. The kinetic data recorded in the PDA mode were only used to qualitatively evaluate spectral changes but not to obtain kinetic constants. Inadvertent photoreduction of 5-deazaFAD in the PDA mode was avoided by attenuating the intensity of the probe beam by ~50%. As a result, the signal-to-noise ratio of the spectra was adversely affected. To enhance the signal-to-noise ratio, each spectrum recorded in the PDA mode was smoothed by averaging five adjacent data points in the original data set to give the final spectrum.

Synthesis of the Internal Standard Norbenzphetamine-d_5. To quantitate norbenzphetamine, it was necessary to synthesize an internal standard. The norbenzphetamine was synthesized as previously described with the following modifications (*22*). In a typical reaction, amphetamine sulfate (2.7 mmol) was dissolved in 2 mL of pyridine to which 3 mL of 6.9 mmol of benzoyl-d_5 chloride in benzene was added dropwise at room temperature over 15 min. The norbenzphetamine synthesis used benzoyl chloride. The reaction mixture was stirred at room temperature for 1 h and then at 60 °C for 30 min. *N*-Benzoylamphetamine-d_5 was first extracted with dichloromethane and then crystallized from the concentrated dichloromethane. The yield of this step was ~25%. Next, the *N*-benzoylamphetamine-d_5 (1.7 mmol) was dissolved in 17 mL of tetrahydrofuran. Over a period of 30 min the *N*-benzoylamphetamine-d_5 solution was added under nitrogen to $LiAlH_4$ (6.5 mmol) dissolved in 7.5 mL of tetrahydrofuran. The reaction mixture was refluxed overnight under nitrogen and terminated by addition of a solution of 90% tetrahydrofuran and 10% water. The mixture was filtered and then extracted with ether. Norbenzphetamine-d_5 was purified by recrystallization from hot ethanol (50 °C) as the hydrochloride salt (mp 174−175 °C). The yield of this step was ~43% for an overall yield of ~11%. The chemical identity of norbenzphetamine-d_5 was confirmed by NMR and by LC-MS/MS which demonstrated the expected daughter ions.

The NMR spectrum was obtained from an ~1 mM solution of norbenzphetamine and its deuterated analogue. The appropriate solution was prepared by dissolving the free base ($C_{16}H_{19}N$) in 99.9% D_2O containing 0.1 M DCl. A proton spectrum was recorded using the water proton as a reference on a Bruker 500 MHz NMR spectrometer. The chemical shifts and coupling constants are given for norbenzphetamine. The ^1H NMR spectrum for norbenzphetamine-d_5 was similar to the norbenzphetamine spectrum except for the expected decrease in five protons and other changes characteristic of a deuterated compound. ^1H NMR at room temperature (δ = ppm): 7.39−7.19 (multiplet, 10H, phenyl), 4.23 [doublet, 1H, PhC**H**$_2$N, J(H,H) = 13.2 Hz], 4.16 [doublet, 1H, PhC**H**$_2$N, J(H,H) = 13.2 Hz], 3.53 [doublet, 1H, PhCH_2C**H**, J(H,H) = 6.65 Hz], 3.11 [doublet, 1H, PhC**H**$_2$CH, J(H,H) = 5.5 Hz], 2.81(doublet, 1H, PhC**H**$_2$-CH, J(H,H) = 8.74 Hz], 1.23 [doublet, 3H, C**H**$_3$, J(H,H) = 6.5 Hz]. These chemical shifts and coupling constants are consistent with those reported for norbenzphetamine in $CDCl_3$ (*23*). A total of 18 protons can be assigned. The N−H proton has been replaced by deuterium.

Quantitation of Norbenzphetamine by LC-MS/MS. Samples for LC-MS/MS analyses were prepared from reactions performed in parallel to the kinetic studies in the stopped-flow spectrophotometer. After reduction of the cyt P450−cyt b_5 or cyt P450−5-deazaFAD reductase complex, by dithionite, 100 μL of the reduced complex was mixed with an equal volume of air-saturated buffer A to initiate the catalysis. As a control, 100 μL of the reduced complex in the appropriate control solution was mixed with an equal volume of anaerobic 2 M H_3PO_4 (2 M) to inactivate the enzymes. Aliquots of 40 μL of the control and reaction mixture were then spiked with 2 ng of norbenzphetamine-d_5, mixed with 0.2 mL of 2 M ammonia, and extracted with 2 mL of *tert*-butyl methyl ether. The extracts were dried with an Alltech vacuum manifold (Alltech) and redissolved in 300 μL of a 10% methanol aqueous solution containing 0.1% formic acid. The amount of norbenzphetamine in the samples was determined from a standard curve constructed by adding 2 ng of norbenzphetamine-d_5 and 0−100 ng of unlabeled norbenzphetamine to a solution containing all of the components of the reaction mixture including the proteins and benzphetamine. The standard curve was linear from 0 to 100 ng (0−0.44 nmol) of norbenzphetamine.

Quantitative analysis of norbenzphetamine was performed on an electrospray mass spectrometer (Micromass Quattro II, Micromass) coupled with a Waters 2690 HPLC system. A reverse-phase C18 column (100 mm × 2 mm, Thermo-Hypersil Keystone Prism) was used for chromatography of the analyte. The column was equilibrated with 0.1% formic acid in water. An aliquot of 25 μL of the analyte sample was injected onto the column and eluted with 0.1% formic acid in methanol at a flow rate of 0.3 mL/min. The benzphetamine and norbenzphetamine both eluted at 4.2 min. However, for quantitative analyses of norbenzphetamine, only the parent ion (*m*/*z* 226.2) of norbenzphetamine and parent ion (*m*/*z* 231.2) of norbenzphetamine-d_5 were admitted to the collision chamber of the mass spectrometer where they were fragmented after colliding with nitrogen molecules. The fragment ions of *m*/*z* 91.2 and *m*/*z* 96 from parent ions of *m*/*z* 226.2 and *m*/*z* 231.2, respectively, were used to establish the standard curve and quantify the amount of norbenzphetamine formed in the single turnover experiments. The pattern of fragment ions indicated that norbenzphetamine and its deuterated analogue were being quantitated.

Miscellaneous. The metabolism of benzphetamine at 15 °C under steady-state conditions was determined by measuring formaldehyde formation using Nash's reagent as previously described (*24*).

RESULTS

Autoxidation of Oxyferrous Cyt P450 2B4. To ensure accurate assignment of each kinetic component during the course of electron transfer from 2-electron-reduced 5-deazaFAD reductase to oxyferrous cyt P450, the kinetics of the autoxidation of oxyferrous cyt P450 were characterized with stopped-flow spectrophotometry. Figure 1 shows the characteristic spectra of ferrous, oxyferrous, and ferric cyt P450 in the presence of 1 mM benzphetamine and the transient absorbance changes at 438 nm following rapid mixing of ferrous cyt P450 with air-saturated buffer. As shown in Figure 1A, the peak absorbance of oxyferrous cyt P450 (solid line) is red shifted to 420 nm compared to the spectra of ferrous and ferric cyt P450, but it is consistent with the spectra of other oxyferrous cyts P450 reported in the literature (*6*, *25*, *26*). Figure 1B illustrates the change in absorbance at 438 nm following the rapid mixing of ferrous cyt P450 2B4 with air-saturated buffer. The majority of oxyferrous cyt P450 is formed in the dead time of the stopped-flow spectrophotometer, and its formation is complete ∼20−30 ms after introduction of oxygen. The second-order rate constant for oxyferrous cyt P450 formation in the presence of benzphetamine is 2.5×10^6 M^{-1} s^{-1} at 15 °C (inset, Figure 1B). This rate constant is comparable with a value of 5×10^5 M^{-1} s^{-1} reported for oxyferrous cyt $P450_{LM4}$ at 10 °C (*26*).

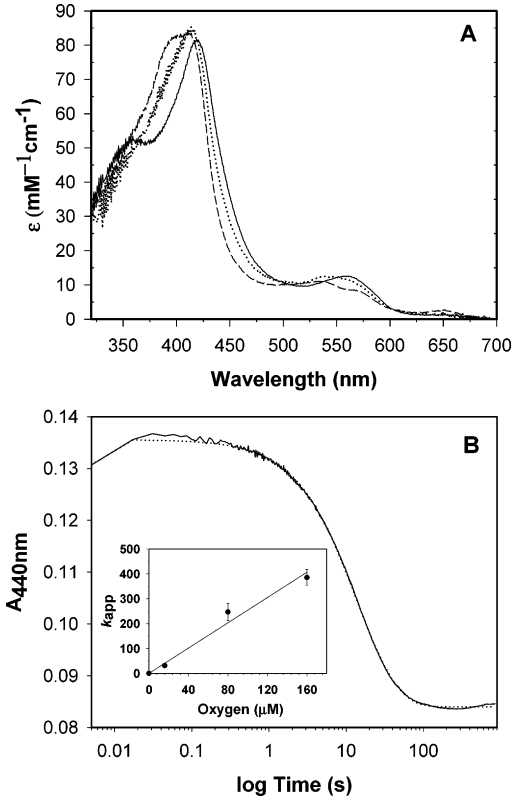

FIGURE 1: Kinetics of autoxidation of cyt P450 2B4 in the presence of 1 mM benzphetamine at 15 °C. (A) Absorbance spectra showing ferrous cyt P450 (dotted line), oxyferrous cyt P450 (solid line), and ferric cyt P450 (60% high spin) (dashed line). The spectrum of ferrous cyt P450 (dotted line) was recorded using the photodiode array mode following mixing of ferrous cyt P450 with anaerobic buffer B, whereas ferric cyt P450 was recorded at 200 s with a photodiode array detector following rapid mixing of ferrous cyt P450 with air-saturated buffer B. The spectrum of oxyferrous cyt P450 was deduced from a 3D kinetic datum set using global analysis software (Spectrum Software Associates). (B) Absorbance changes at 438 nm recorded in photomultiplier mode (solid line). The fitting is depicted with a dotted line. Inset: Determination of the second-order rate constant for the formation of oxyferrous cyt P450. Various oxygen concentrations were obtained by diluting air-saturated buffer B with anaerobic buffer B. Apparent rate constants k_{app} were obtained by fitting the initial absorbance changes at 438 nm with a single exponential function.

At 15 °C oxyferrous cyt P450 is unstable and spontaneously decays to generate ferric cyt P450 and a superoxide anion, leading to a decrease in absorbance at 438 nm. As shown in Figure 1B, decay of oxyferrous cyt P450 in the presence of 1 mM benzphetamine is biphasic and considerably slower than its formation. The kinetics of oxyferrous

Table 1: Summary of Rate Constants and Amplitudes for Autoxidation and Redox Reactions of Cyt P450, Cyt b_5, and 5-DeazaFAD Reductase in the Absence and Presence of Their Redox Partners

syringe 1	syringe 2	λ (nm) obs[a]	species obs[a]	phase 1		phase 2		phase 3	
				A (%)	k_1 (s^{-1})	A (%)	k_2 (s^{-1})	A (%)	k_3 (s^{-1})
2e-reduced 5-deazaFAD reductase[c]	O_2	450	reductase					100 ± 11	0.007 ± 0.001
		585	reductase					100 ± 8	0.007 ± 0.001
cyt b_5^{2+}	O_2	422	cyt b_5					97 ± 5	0.005 ± 0.0003
$P450^{2+}$	O_2	438	P450	25 ± 3	0.96 ± 0.2	34 ± 6	0.13 ± 0.04	41 ± 7	0.016 ± 0.005
$P450^{2+}$ + 1 mM BP[b]	O_2 + 1 mM BP	438	P450			40 ± 4	0.13 ± 0.05	60 ± 7	0.048 ± 0.004
2e-reduced 5-deazaFAD reductase[c]	cyt b_5^{2+}	422	cyt b_5					98 ± 10	0.002 ± 0.0002
		567	reductase					100 ± 12	0.002 ± 0.0004
$P450^{2+}$−cyt b_5^{2+} + 1 mM BP	O_2 + 1 mM BP	422	cyt b_5	50 ± 6	9.3 ± 0.7	4 ± 0.1	0.43 ± 0.21	46 ± 7	0.005 ± 0.0003
		438	P450	62 ± 7	10.5 ± 1.5	18 ± 1.1	0.83 ± 0.18	20 ± 3	0.005 ± 0.001
$P450^{2+}$−2e-reduced 5-deazaFAD reductase + 1 mM BP	O_2 + 1 mM BP	598	reductase	31 ± 6	8.4 ± 1.5	52 ± 6	0.37 ± 0.06	17 ± 0.7	0.041 ± 0.005
		438	P450			86 ± 10	0.090 ± 0.01	14 ± 0.5	0.012 ± 0.002

[a] Observed. [b] Benzphetamine. [c] These data are from ref *16*.

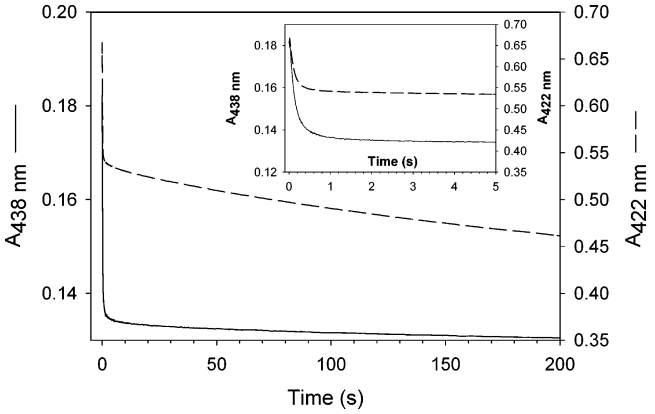

FIGURE 2: Kinetics of the reduction of oxyferrous cyt P450 2B4 by cyt b_5. The final concentration of cyt P450 and cyt b_5 in the observation cuvette was 5 μM. The solid and dashed lines represent absorbance changes observed at 438 nm (P450) and 422 nm (b_5), respectively. The experiments were performed as described in Materials and Methods.

cyt P450 autoxidation at 438 nm can be fitted with two exponentials with rate constants of 0.13 and 0.048 s^{-1} (Table 1). The fast phase constitutes approximately 40% of the overall amplitude, while the slow phase constitutes the remaining 60%. Overall, 50% of oxyferrous cyt P450 decays within 10 s. A spectrum recorded 200 s following introduction of oxygen is characteristic of ferric cyt P450 (dashed line of Figure 1A) with a charge transfer band at 650 nm. In the absence of substrate cyt P450 2B4 autoxidizes more rapidly with triphasic kinetics and a half-life of 2.2 s (see Table 1), suggesting that the substrate stabilizes oxyferrous cyt P450 2B4.

Electron Transfer from Ferrous Cyt b_5 to Oxyferrous Cyt P450 2B4. As a control, the rate of the second electron transfer from ferrous cyt b_5 to oxyferrous cyt P450 was measured at 15 °C, and the results are presented in Figure 2. Oxyferrous cyt P450 and cyt b_5 were followed at 438 nm (solid line) and 422 nm (dashed line), respectively. The absorbance change observed at 438 nm arises exclusively from oxyferrous cyt P450 as this is an isosbestic point for cyt b_5 (*27*). At 422 nm ~90% of the absorbance change arises from cyt b_5 and ~10% reflects the formation and subsequent decay of oxyferrous cyt P450 (see Figure 1A). Oxyferrous cyt P450 forms within ~20−30 ms as evidenced by the initial increase in absorbance (Figure 2). Subsequently, the absorbance at both wavelengths decreases rapidly and simultaneously, indicating that intermolecular electron transfer has occurred without formation of an observable intermediate. The overall kinetics at both wavelengths are multiphasic. Fitting of the kinetic traces reveals that oxyferrous cyt P450 decays with rate constants of 10.5, 0.83, and 0.005 s^{-1}, whereas ferrous cyt b_5 oxidizes with rate constants of 9.3, 0.043, and 0.005 s^{-1} (Table 1). The fast phase of this reaction with a rate constant of ~10 s^{-1} is attributed to electron transfer from ferrous cyt b_5 to oxyferrous cyt P450. This rapid rate of oxidation of both redox proteins is 100−2000-fold faster than the autoxidation of the individual proteins (Table 1). Other investigators have reported similar values for the rate of the second electron transfer from ferrous cyt b_5 to microsomal cyt P450 at 2 °C (*10*, *12*). The more rapid oxidation of cyt P450 compared to cyt b_5 after the fast phase may be partly attributed to electron transfer from oxyferrous cyt P450 to the ferric cyt b_5 which is generated in the first phase of the reaction. Separate experiments in this laboratory and by other investigators indicate that this reaction occurs at a rate of ~2−3 s^{-1} at a cyt b_5:cyt P450 2B4 molar ratio of 1:1 (*12*).

Electron Transfer from 2-Electron-Reduced 5-DeazaFAD T491V Reductase to Oxyferrous Cyt P450 2B4. A detailed description of the preparation and characterization of 5-deazaFAD T491V reductase has been published (*16*). For the experiments described here it is important to be cognizant of the fact that the 5-deazaFAD cofactor remains in the fully oxidized state during the course of the experiments with cyt P450 and that in control experiments the 5-deazaFAD T491V reductase transfers a single electron from the FMN hydroquinone to cyt *c* and cyt b_5 in a manner indistinguishable from that of wild-type reductase. The rate of electron transfer from 5-deazaFAD reductase to oxyferrous cyt P450 was measured by mixing the preformed 1:1 ferrous cyt P450−2-electron-reduced 5-deazaFAD reductase complex with air-saturated buffer and following the absorbance changes spectrophotometrically. The complex was reduced stoichiometrically by titrating with dithionite (Figure 3). The spectrum of the oxidized complex shows the $\alpha\beta$ bands of the heme near 550 nm, a charge-transfer band at 650 nm from high-spin ferric cyt P450, and a shoulder at 480 nm from the FMN cofactor of the reductase (solid line of Figure 3). Addition of dithionite led to an increase in absorbance at 550 nm and decrease in absorbance at 650 nm (reflecting formation of the reduced cytochrome) and a decrease in absorbance at 480 nm due to reduction of FMN. Reduction

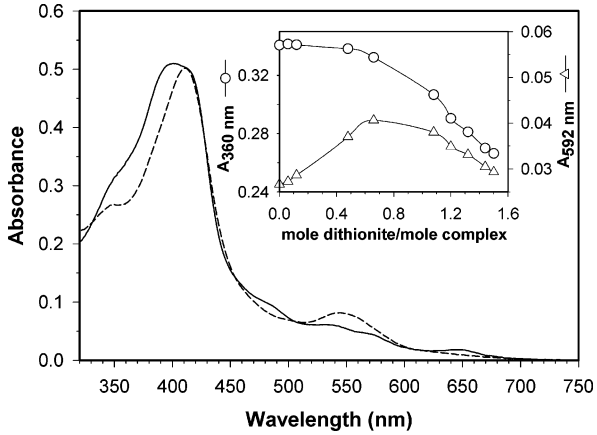

FIGURE 3: Reduction of the cyt P450−5-deazaFAD reductase complex by stoichiometric amounts of dithionite. Cyt P450 and 5-deazaFAD reductase (5 μM) were incubated overnight at 4 °C to preform the protein complex as described in Materials and Methods. Prior to titration, 1 mM benzphetamine and 0.1 μM methyl viologen were added to the protein complex. The solid and dashed lines represent the spectra of the complex at the beginning and at the end of the titration, respectively. Inset: Absorbance changes at 592 nm (open triangle) and 360 nm (open circle) during the course of the titration.

of cyt P450 and 5-deazaFAD reductase was monitored at 360 and 592 nm, respectively, as the former is an isosbestic point for the reductase and the latter is an isosbestic point for cyt P450. As shown in the inset of Figure 3 (open triangle), the absorbance due to FMNH$^\bullet$ at 592 nm increases with the addition of dithionite and reaches a maximum when ~0.6 electron equiv has been added. Further addition of dithionite led to a decrease in absorbance at 592 nm due to formation of the FMN hydroquinone.

Reduction of ferric cyt P450 was followed at 360 nm (Figure 3). The absorbance at 360 nm did not change significantly until the FMN had been converted to its semiquinone, indicating that reduction of ferric cyt P450 did not occur until FMN was reduced to FMNH$^\bullet$ as expected since the potential of the FMN/FMNH$^\bullet$ couple is −110 mV (*28*). Further addition of dithionite led to a decrease in absorbance at both 592 and 360 nm, indicating that both the ferric iron of the heme and the FMNH$^\bullet$ of the reductase were being reduced simultaneously. Following addition of 3 electron equiv the protein complex showed spectral features characteristic of a reduced complex, with a red-shifted Soret band and disappearance of both the shoulder at 480 nm and the charge-transfer band at 650 nm. Since the potential of the FMN semiquinone/hydroquinone couple is known (−270 mV) and the concentration of the reduced form of cyt P450 and FMN could be accurately measured during the titration, it was possible to use eq 1 to estimate the potential of cyt P450 2B4 in the presence of 1 mM benzphetamine and cyt P450 reductase (*28*). At equilibrium, the redox potential of cyt P450 at 20 °C is given by

$$E^0_{P450} = E^0_{SQ/HQ} + 0.057 \log\left(\frac{[P450^{2+}][SQ]}{[P450^{3+}][HQ]}\right) \quad (1)$$

where [SQ], [HQ], [$P450^{2+}$], and [$P450^{3+}$] represent the concentration of FMNH$^\bullet$, $FMNH_2$, ferrous cyt P450, and ferric cyt P450, respectively. The redox potential of cyt P450 2B4 in the presence of 1 mM benzphetamine at 20 °C was calculated to be −245 mV, in agreement with the published value (*29*). In the absence of substrate and the reductase the potential of cyt P450 2B4 is ~−330 mV (*11*). The decrease in potential of cyt P450 2B4 upon binding substrate enables it to accept an electron from reductase.

Figure 4 shows the transient absorbance changes in the presence of benzphetamine at 598 and 438 nm following the rapid mixing of the reduced complex with air-saturated buffer. The reductase was followed at 598 nm as this is an isosbestic point for the oxyferrous/ferric cyt P450 couple, whereas oxyferrous cyt P450 was followed at 438 nm. At this wavelength 87% of the absorbance decrease can be attributed to the oxidation of cyt P450 while 13% is due to the oxidation of the reductase (*16*). At ~30 ms following introduction of oxygen when oxyferrous cyt P450 has formed, there is a sharp increase in absorbance at 598 nm representing the rapid oxidation of ≅30% of the $FMNH_2$ to FMNH$^\bullet$. By 1 s ~50% of the reductase has oxidized whereas virtually none of the oxyferrous cyt P450 has returned to the ferric state. It is apparent from the kinetic trace at 598 nm that the oxidation of the $FMNH_2$ is multiphasic. Three exponential phases can be fitted to the kinetic trace at 598 nm, giving rate constants of 8.4, 0.37, and 0.041 s^{-1}. The relative amplitudes for these phases are 31%, 52%, and 17%, respectively (Table 1). All three of these phases are

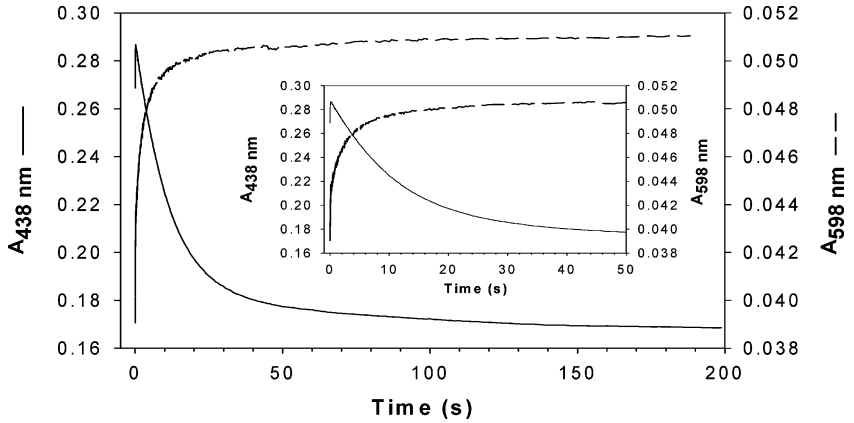

FIGURE 4: Kinetics of reduction of oxyferrous cyt P450 2B4 by 5-deazaFAD reductase. The final concentration of cyt P450 and 5-deazaFAD reductase in the observation cell of the stopped-flow spectrophotometer was 4.7 μM. The solid and dashed lines represent absorbance changes observed at 438 nm (cyt P450) and 598 nm (reductase), respectively. The experiment was performed as described in Materials and Methods.

significantly faster than the autoxidation of 5-deazaFAD reductase ($k = 0.007$ s^{-1}), which suggests that all of the reductase molecules may have transferred an electron to a cyt P450 molecule (Table 1, Figure 4) (*16*). Further investigation will be required to identify the processes responsible for the different phases of reductase oxidation.

Remarkably, the kinetic trace at 438 nm does not parallel the trace at 598 nm; rather it is characterized by a small increase in absorbance (solid line of Figure 4) in the first 20 ms similar to the increase in absorbance seen in cyt P450 in Figures 1 and 2. This initial rapid increase in absorbance at 438 nm reports on the formation of oxyferrous cyt P450. Oxyferrous cyt P450 only begins to revert to the ferric protein after a time lag of ~1 s with a rate constant of 0.09 ± 0.01 s^{-1}, by which time 50% of the reductase has oxidized. This phase accounts for $86 \pm 10\%$ of the absorbance change in oxyferrous cyt P450 (Table 1). Figure 4 clearly illustrates that cyt P450 and the 2-electron-reduced 5-deazaFAD reductase undergo spectral changes at dissimilar rates. It was expected that upon receiving the electron from the reductase oxyferrous cyt P450 would be reduced and then immediately undergo catalytic turnover to generate product and ferric cyt P450 as it does in the presence of cyt b_5 (Figure 2). This did not occur. The results have been interpreted to indicate that the reductase oxidizes to the 1-electron-reduced $FMNH^{\bullet}$ air-stable semiquinone while the cyt P450 forms an intermediate with a spectrum similar to that of oxyferrous cyt P450. Only ~1 s after mixing with oxygen does the absorbance at 438 nm begin to decrease biphasically (see Table 1).

The spectral changes occurring following rapid mixing of the cyt P450−5-deazaFAD reductase complex with oxygen were also examined between 330 and 700 nm using a photodiode array detector. A total of 160 spectra were recorded every 50 ms in the stopped-flow spectrophotometer on a log time scale. Four typical spectra are presented in Figure 5A. Spectrum 1 (dotted line of Figure 5A) of the reduced complex was recorded under anaerobic conditions prior to mixing with oxygen. After rapid mixing of the reduced protein complex with oxygen, the very first spectrum or spectrum 2 (short dashed line of Figure 5A) was recorded at ~125 ms. Due to the spectrophotometer software the absolute timing of this spectrum is uncertain as the timing of the first data point varies with the length of data acquisition, integration time of the photodiode array detector, number of data points, etc. Thus, it is not possible to precisely compare the absolute time for the kinetic traces recorded in the different spectrometer detection modes. Nonetheless, the rate constants and amplitudes of the kinetic traces should not be significantly affected.

The Soret and $\alpha\beta$ bands of spectrum 2 are clearly red shifted compared to spectrum 1, and a new peak appears at 350 nm. These spectral changes at the initial phase of the reaction indicate that oxyferrous cyt P450 has formed. The net spectral changes due to formation of oxyferrous cyt P450 are demonstrated in the difference spectrum (spectrum 2 minus spectrum 1) presented in Figure 5B (solid line). The peak at 438 nm and trough at 390 nm in the difference spectrum are characteristic of formation of oxyferrous cyt P450 from ferrous cyt P450. Interestingly, no significant spectral changes occur in the range of 600−700 nm where ferric cyt P450 and $FMNH^{\bullet}$ absorb. This indicates that neither ferric cyt P450 nor $FMNH^{\bullet}$ was formed at this time. Thus,

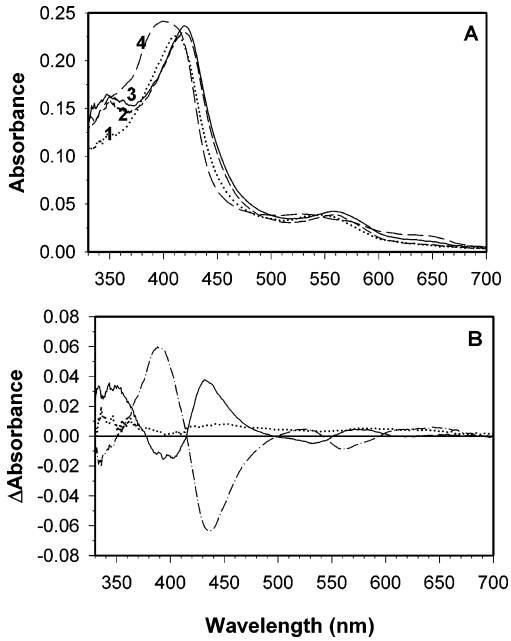

FIGURE 5: UV−visible and difference spectra of the oxyferrous cyt P450 2B4−5-deazaFAD complex. The spectra were recorded with a photodiode array detector after rapid mixing of the 3-electron-reduced cyt P450−5-deazaFAD reductase complex with air-saturated buffer at 15 °C. The final concentration of cyt P450 and 5-deazaFAD reductase in the observation cell of the spectrophotometer was 2.5 μM; the benzphetamine concentration was 1 mM. (A) Spectrum 1 (dotted line) is the spectrum of the reduced cyt P450−5-deazaFAD reductase complex recorded under anaerobic conditions; spectrum 2 (short dashed line) is the first spectrum of the 160 transient spectra ~125 ms after mixing; spectrum 3 (solid line) was recorded 2 s after mixing; spectrum 4 (long dashed line) was recorded at 237.5 s. (B) Difference spectra generated from the spectra in panel A: solid line, spectrum 2 minus spectrum 1; dotted line, spectrum 3 minus spectrum 2; dashed line, spectrum 4 minus spectrum 3.

spectrum 2 is representative of oxyferrous cyt P450 and the 2-electron-reduced 5-deazaFAD reductase.

Spectrum 3 in Figure 5A (solid line) recorded at 2 s shows a significant absorbance increase from 410 to 660 nm, particularly around 438 and 585 nm. This is more clearly illustrated in the difference spectrum (spectrum 3 minus spectrum 2) presented in Figure 5B (dotted line). The broad increase in absorbance is indicative of oxidation of the reductase from $FMNH_2$ to the air-stable $FMNH^{\bullet}$. No significant spectral changes occur that can be attributed to formation of ferric cyt P450, which should lead to a large decrease in absorbance at 438 nm. In other words, oxyferrous cyt P450 and/or its reduced intermediate do (does) not convert to ferric cyt P450 at the same rate as $FMNH_2$ is oxidized to $FMNH^{\bullet}$. Formation of ferric cyt P450 does, however, occur as indicated by spectrum 4 (Figure 5A, long dashed line) recorded ~240 s after introduction of oxygen. Formation of ferric cyt P450 at ~240 s is illustrated in the difference spectrum (spectrum 4 minus spectrum 3) in Figure 5B (long dashed line) where a pair of peaks are observed at 385 and 438 nm. The increase in absorbance at 385 nm is consistent with formation of high-spin ferric cyt P450, whereas the decrease in absorbance at 438 nm indicates a decrease in oxyferrous and/or the 1-electron-reduced cyt P450 intermediate. Global analysis of the spectral changes did not reveal the presence of any intermediates.

Table 2: Efficiency of Cyt P450 2B4 Catalysis in the Presence of Cyt b_5 and 5-DeazaFAD T491V Reductase

protein complex (5 μM)	norbenzphetamine (μM)[a]	efficiency (%)
cyt P450 + cyt b_5	2.6 ± 0.42	52.0 ± 8.4
cyt P450 + 5-deazaFAD reductase	1.6 ± 0.14	32.0 ± 2.8

[a] The amount of product, norbenzphetamine, formed in the single turnover experiment was determined by LC-MS/MS as described in Materials and Methods. The results are presented as an average of three values with the standard deviation.

At 15 °C the steady-state rate of benzphetamine metabolism by cyt P450 2B4 is 5 nmol of formaldehyde formed (nmol of P450)$^{-1}$ min^{-1}, which indicates that the rate constant for cyt P450 catalysis is 0.08 s^{-1}. Thus the rate of decay of oxyferrous cyt P450 2B4 ($k = 0.09$ s^{-1}) determined under pre-steady-state conditions in the stopped-flow spectrophotometer (Table 1) and the rate of metabolism of benzphetamine under steady-state conditions are the same within experimental error.

Quantitation of Norbenzphetamine under Single Turnover Conditions. To confirm that catalysis was occurring under the single turnover experimental conditions, a sensitive assay for norbenzphetamine was developed. A linear calibration curve using the internal standard norbenzphetamine-d_5, which has one of its benzene rings perdeuterated, was constructed with 0−100 ng of norbenzphetamine. Table 2 illustrates that the product, norbenzphetamine, was formed with 52% efficiency in the presence of cyt b_5 but with only 32% efficiency in the presence of 5-deazaFAD reductase. These results under single turnover conditions confirm our findings under steady-state conditions where it could be demonstrated that cyt b_5 increased product formation by approximately 20% primarily by decreasing superoxide production (*13*).

DISCUSSION

It has been possible for the first time to directly measure the rate of reduction of an oxyferrous microsomal cyt P450 by a cyt P450 reductase and its subsequent turnover to ferric cyt P450 with product formation. These experiments demonstrate that in the presence of cyt P450 reductase catalysis by oxyferrous cyt P450 2B4 proceeds via a long-lived reduced intermediate with an absorption spectrum apparently similar to that of oxyferrous cyt P450. Global analysis of the spectral data obtained with the photodiode array detector was unable to detect a new spectral intermediate. In theory, the intermediate could be the reduced oxyferrous cyt P450 $(Fe^{3+}OO)^{2-}$, some species further along the reaction cycle, such as the hydroperoxo species $(Fe^{3+}OOH)^{-}$, or a previously unidentified ephemeral compound such as an oxidized substrate−heme complex. A hydroperoxo-like species would be more stable than the very nucleophilic peroxo species which Sligar and co-workers have demonstrated has an absorbance maximum at 440 nm (*6*). Dr. D. Harris has calculated (personal communication) that oxyferrous cyt P450 and the hydroperoxo intermediate have similar absorption spectra while the peroxo intermediate has a red-shifted Soret peak, in agreement with experimental results. The rate of turnover of oxyferrous cyt P450 in the presence of the 2-electron-reduced 5-deazaFAD reductase ($k = 0.09$ s^{-1}) is similar to the rate of product formation under steady-state conditions at the same temperature, 15 °C. In striking contrast the reduction of oxyferrous cyt P450 2B4 by ferrous cyt b_5 proceeds with the ~100-fold more rapid ($k = 10.5$ s^{-1}) return of oxyferrous cyt P450 to the ferric resting state. Product is generated in the presence of both cyt b_5 and 5-deazaFAD reductase under these single turnover conditions with an efficiency of 52% and 32%, respectively. An ≅20% increase in the efficiency of BP metabolism by cyt 2B4 has also been observed under steady-state conditions when cyt b_5 is present (*13*).

These results assume that the FMN domain of the T491V mutant cyt P450 reductase which has been reconstituted with the nonphysiologic flavin, 5-deazaFAD, behaves in a manner identical to that of the wild-type protein. Unfortunately, this assumption cannot be rigorously tested since the spectral changes in the wild-type diflavin reductase are too complex to deconvolute under the experimental conditions due to the rapidly equilibrating different flavin redox states. In fact, the inability to unambiguously interpret the spectral changes that the wild-type cyt P450 reductase undergoes during its electron transfer reactions prompted us to prepare the 5-deazaFAD T491V reductase with only a single functioning flavin so that it would be possible to monitor transfer of electrons from the FMN hydroquinone to its protein redox partners. Nonetheless, we believe the T491V mutation, which to the best of our knowledge only decreases the affinity of FAD for the reductase by disrupting a hydrogen bond between threonine 491 and a phosphate of FAD, does not cause functional changes in the FMN domain. As the 5-deazaFAD T491V reductase reduces cyt *c* and the amphipathic cyt b_5 at the same rate as the wild-type reductase, it is likely that it also interacts with oxyferrous cyt P450 2B4 in a manner identical to that of the wild-type protein.

The experiments reported herein partly explain the long-standing puzzling observation that in liver microsomes under steady-state conditions an intermediate with an absorption spectrum similar to that of oxyferrous cyt P450 accumulates. In his prescient studies Estabrook demonstrated that cyt b_5 was able to decrease the concentration of this intermediate and concluded that this intermediate was relevant to the rate-limiting step of catalysis (*30*). Guengerich and co-workers using purified human cyt P450 2D6 have recently confirmed that a cyt P450 intermediate with a spectrum similar to that of oxyferrous cyt P450 accumulates under steady-state turnover conditions. Simulation of their kinetic data yielded a catalytic mechanism limited by the rate of protonation of a reduced oxyferrous intermediate and subsequent O−O bond scission and rate of cleavage of the C−H bond (*4*). Thus our experiments performed under pre-steady-state conditions are consistent with what is observed under steady-state conditions. The unanticipated findings also contribute to our understanding of the long-standing question: how does cyt b_5 increase the efficiency of cyt P450 catalysis under steady-state conditions in the presence of cyt P450 reductase? Since cyt P450 2B4 turnover is so rapid when cyt b_5 delivers the second electron, this reaction competes favorably with the less efficient turnover catalyzed by the more tightly binding cyt P450 reductase which has a greater affinity for cyt P450 2B4 than cyt b_5 (*13*, *31*).

The observation that catalysis in the presence of cyt b_5 and 5-deazaFAD reductase (and presumably wild-type cyt P450 reductase) proceeds at markedly different rates raises

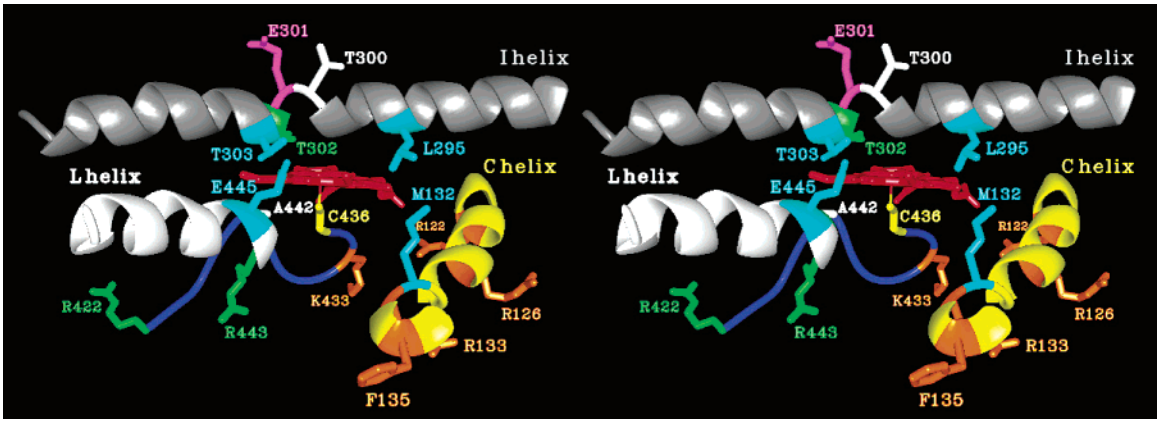

FIGURE 6: Stereo overview of the structure of the proximal and distal faces of the heme in a model of cyt P450 2B4 based on the cyt P450 2C5 crystal structure. The model for cyt P450 2B4 was constructed as previously described for cyt P450 2E1 (*41*). The residues in orange are involved in binding of cyt b_5 and cyt P450 reductase. The residues in green only bind to cyt P450 reductase (*24*). The blue line represents the peptide backbone of residues connecting the meander and β-bulge. Residues M132 and L295 and T303 and E445 are in van der Waals contact.

the intriguing question: what is the molecular basis for the distinctive behavior of oxyferrous cyt P450 in the presence of its two reductants? It is hypothesized that binding of cyt b_5 to the proximal surface of cyt P450 near the heme causes a conformational change on the distal side of the heme that optimizes catalysis and cleavage of the oxygen bond with the generation of the catalytically competent oxyferryl heme which is formed without an energy barrier following delivery of a second proton to the distal oxygen (*32*). Examination of a model of cyt P450 2B4 based on the crystal structure of cyt P450 2C5 indicates that the side chain of Met 132 in the C helix is close to where cyt b_5 binds and, in addition, is in van der Waals contact with Leu 295 in the amino-terminal end of the I helix (Figure 6). Leu 295 is also in van der Waals contact with the heme. Thus it is entirely possible that structural changes occurring in the C helix upon binding of cyt b_5 could produce conformational changes in the I helix near Thr 302. In oxyferrous cyt $P450_{cam}$ Thr 252, the residue homologous to Thr 302, has been shown by X-ray crystallography to hydrogen bond to a water molecule which is in a position to deliver a proton to the peroxo $(Fe^{3+}O_2)^{2-}$ intermediate (*33*).

Experimental support for the notion that cyt b_5 causes a conformational change on the distal side of the heme comes from numerous experiments that demonstrate a marked increase in the high-spin form of ferric cyt P450 in the presence of cyt b_5 (*24*, *34*). The increase in the high-spin form of cyt P450 on binding of cyt b_5 and its enhancement by substrate are attributed to displacement of water as the sixth axial ligand of the heme (*31*). A plausible mechanism for this displacement is suggested by the crystal structure of substrate-bound cyt P450 BM3, which reveals a conformational change in the I helix which allows the axially liganded water molecule to be displaced to a higher affinity binding site 1 Å away. The close proximity of the water molecule to the heme iron suggests that it might be available to participate in the proton delivery pathway (*35*).

Our findings with 5-deazaFAD reductase can be explained by assuming that binding of the reductase to the proximal surface of cyt P450 results in a conformation that slows catalysis possibly by disorganizing the proton delivery pathway and slowing protonation or by a previously undescribed mechanism. If proton delivery which is thermodynamically favorable is delayed, then the 5-deazaFAD reductase induced conformation must be able to temporarily stabilize an otherwise highly reactive intermediate. A second explanation for our results is that the cyt P450 2B4 conformation in the presence of the reductase is incompetent in catalysis and that the rate-limiting step in catalysis is a kinetically gated change in conformation to a catalytically competent conformation. The observation that turnover in the presence of 5-deazaFAD reductase ($k = 0.09\ s^{-1}$) occurs 100-fold more slowly than in the presence of cyt b_5 ($k = 10\ s^{-1}$) suggests significantly different chemical environments on the distal face of the heme. Examination of the stereo model of cyt P450 2B4 in Figure 6 illustrates the location of selected residues known to be involved in binding reductase. A portion of the reductase binding site involving the C and C′ helices of cyt P450 2B4 is situated on the proximal surface near the heme and overlaps the binding site for cyt b_5 (*24*). The remaining portion of the reductase binding site is unique to the reductase and involves cyt P450 2B4 residues Arg 422 between the meander and β-bulge and Arg 443 in the L helix. Figure 6 depicts the location of these residues in relationship to the I helix and Thr 302. Arg 433 is close to Glu 445 which is hydrogen bonded to Thr 303 in the I helix, and it is adjacent to Ala 442 which is in van der Waals contact with the heme. The proximity of the reductase binding site to the heme should provide it with the opportunity to modulate the structure of the proton delivery network and/or the electronic properties of the heme. This proposal is consistent with multidimensional high-resolution NMR experiments demonstrating that putidaredoxin, the physiological reductant of cyt $P450_{cam}$, perturbs residues both near the heme and remote from the putative putidaredoxin binding site (*36*). Compared to cyt b_5, cyt P450 reductase causes a minimal change in spin state of the ferric cyt P450 (*34*, *37*). This observation is consistent with our suggestion that cyt b_5 and cyt P450 reductase have different effects on the structure of the distal side of the heme.

Other interpretations of our findings of a lag time for decay of oxyferrous cyt P450 2B4 with reductase are possible; for example, the $FMNH_2$ cofactor of the reductase may reduce a spectrally silent group on the reductase which subsequently donates the electron to cyt P450. This is considered unlikely in view of the fact that in control experiments 5-deazaFAD

reductase reduced cyt b_5 and cyt *c*, without evidence of an intermediate, and spectral changes occurred simultaneously in the reductase and the cytochromes. Furthermore, when native cyt P450 reductase and other homologous diflavin reductases reduce their redox partners, the flavin has always been observed to directly transfer the electron without an intermediary (*16*, *38*, *39*). Flavodoxins which are homologous to the FMN domain of cyt P450 reductase also directly donate an electron to an acceptor without an intermediate (*40*). A second explanation for the delayed reoxidation of oxyferrous cyt P450 is that there is a spectrally silent second electron acceptor on the oxyferrous cyt P450 which receives the electron from the reductase and then transfers it to the oxyferrous heme. Again, the control experiments with cyt b_5 presented here and published previously suggest that the oxyferrous heme is the direct recipient of the electron (*10*, *12*). A third explanation is that oxyferrous cyt P450 exists in two conformations, one of which binds cyt b_5 and the other binds cyt P450 reductase. Finally, due to the proximity of reductase and cyt b_5 binding sites to the heme, it is not prudent to eliminate the possibility that 5-deazaFAD reductase and cyt b_5 are causing their effects by directly altering the electronic properties of the heme and its thiolate ligand.

ACKNOWLEDGMENT

We are grateful to Carol Chanter for help in preparing the manuscript and Scott Woehler for obtaining the NMR spectra.

REFERENCES

1. Ortiz de Montellano, P. R. (1995) in *Cytochrome P450: Structure, Mechanism and Biochemistry* (Ortiz de Montellano, P. R., Ed.) 2nd ed., pp 245−304, Plenum Press, New York.
2. Guengerich, F. P. (2001) *Chem. Res. Toxicol. 14*, 611−650.
3. White, R. E., and Coon, M. J. (1980) *Annu. Rev. Biochem. 49*, 315−356.
4. Guengerich, F. P., Miller, G. P., Hanna, I. H., Sato, H., and Martin, M. V. (2002) *J. Biol. Chem. 277*, 33711−33719.
5. Davydov, R., Makris, T. M., Kofman, V., Werst, D. E., Sligar, S. G., and Hoffmann, B. M. (2001) *J. Am. Chem. Soc. 123*, 1403−1415.
6. Denisov, I. G., Makris, T. M., and Sligar, S. G. (2001) *J. Biol. Chem. 276*, 11648−52.
7. Brewer, C. B., and Peterson, J. A. (1988) *Arch. Biochem. Biophys. 263*, 791−798.
8. Oprian, D. D., and Coon, M. J. (1982) *J. Biol. Chem. 257*, 8935−8944.
9. Newcomb, M., Hollenberg, P., and Coon, M. (2003) *Arch. Biochem. Biophys. 409*, 72−79.
10. Bonfils, C., Balny, C., and Maurel, P. (1981) *J. Biol. Chem. 256*, 9457−9465.
11. Guengerich, F. P., Ballou, D. P., and Coon, J. J. (1975) *J. Biol Chem. 250*, 7405−7414.
12. Pompon, D., and Coon, M. J. (1984) *J. Biol. Chem. 259*, 15377−15385.
13. Gruenke, L. D., Konopka, K., Cadieu, M., and Waskell, L. (1995) *J. Biol. Chem. 270*, 24707−24718.
14. Canova-Davis, E., Chiang, J. Y., and Waskell, L. (1985) *Biochem. Pharmacol. 34*, 1907−1912.
15. Canova-Davis, E., and Waskell, L. (1984) *J. Biol. Chem. 259*, 2541−2546.
16. Zhang, H., Gruenke, L., Saribas, A. S., Im, S.-C., Shen, A. L., Kasper, C. F., and Waskell, L. (2003) *Biochemistry 42*, 6804−6813.
17. Shen, A. L., and Kasper, C. B. (2000) *J. Biol. Chem. 275*, 41087−41091.
18. Saribas, A. S., Gruenke, L. D., and Waskell, L. (2001) *Protein Expression Purif. 21*, 303−309.
19. Mulrooney, S. B., and Waskell, L. (2000) *Protein Expression Purif. 19*, 173−178.
20. Omura, T., and Sato, R. (1964) *J. Biol. Chem. 239*, 2370−2378.
21. Estabrook, R. W., and Werringloer, J. (1978) *Methods Enzymol. 52*, 212−220.
22. Hodek, P., and Strobel, H. W. (1994) *Bioorg. Chem. 22*, 253−267.
23. Hartung, C. G., Breindl, C., Tillack, A., and Beller, M. (2000) *Tetrahedron 56*, 5157−5162.
24. Bridges, A., Gruenke, L., Chang, Y. T., Vakser, I. A., Loew, G., and Waskell L. (1998) *J. Biol. Chem. 273*, 17036−17049.
25. Bonfils, C., Debey, P., and Maurel, P. (1979) *Biochem. Biophys. Res. Commun. 88*, 1301−1307.
26. Lambeir, A. M., Appleby, C. A., and Dunford, H. B. (1985) *Biochim. Biophys. Acta 828*, 144−150.
27. Strittmatter, P., and Velick, S. F. (1956) *J. Biol. Chem. 221*, 253−264.
28. Vermilion, J. L., and Coon, M. J. (1978) *J. Biol. Chem. 253*, 8812−8819.
29. Lewis, D. F. V. (1996) in *Cytochromes P450*, p 102, Taylor and Francis, Bristol.
30. Hildebrandt, A., and Estabrook, R. W. (1971) *Arch. Biochem. Biophys. 143*, 66−79.
31. Schenkman, J. B., and Jansson, I. (2003) *Pharmacol. Ther. 97*, 139−152.
32. Harris, D. L., and Loew, G. H. (1998) *J. Am. Chem. Soc. 120*, 8941−8948.
33. Schlichting, I., Berendzen, J., Chu, K., Stock, A. M., Maves, S. A., Benson, D. E., Sweet, R. M., Ringe, D., Petsko, G. A., and Sligar, S. G. (2000) *Science 287*, 1615−1622.
34. Tamburini, P., and Gibson, G. (1983) *J. Biol. Chem. 258*, 13444−13452.
35. Haines, D. C., Tomchick, D. R., Machius, M., and Peterson, J. A. (2001) *Biochemistry 40*, 13456−13465.
36. Pochapsky, S. S., Pochapsky, T. C., and Wei, J. W. (2003) *Biochemistry 42*, 5649−5656.
37. French, J. S., Guengerich, F. P., and Coon, M. J. (1980) *J. Biol. Chem. 255*, 4112−4119.
38. Strobel, H. W., Hodgson, A. V., and Shen, S. (1995) in *Cytochrome P450: Structure, Mechanism and Biochemistry*, 2nd ed., p 225, Plenum Press, New York.
39. Wolthers, K., Basran, J., Munro, A., and Scrutton, N. (2003) *Biochemistry 42*, 3911−3920.
40. Ludwig, M., and Luschinsky, C. L. (1992) Structure and redox properties of clostridial flavodoxins, in *Chemistry and Biochemistry of Flavoenzymes* (Mueller, F., Ed.) Vol. 3, pp 427−466, CRC Press, Boca Raton, FL.
41. Park, J.-Y., and Harris, D. (2003) *J. Med. Chem. 46*, 1645−1660.

BI034968U